International Journal of Precision Engineering and Manufacturing (2020) 21:249–256
https://doi.org/10.1007/s12541-019-00240-8

Online ISSN 2005-4602
Print ISSN 2234-7593

REGULAR PAPER

Design and Analysis of Artificial Muscle Robotic Elbow Joint Using Shape Memory Alloy Actuator

Hyung-Bin Park[1] · Dong-Ryul Kim[1] · Hyung-Jung Kim[1] · Wei Wang[3] · Min-Woo Han[2] · Sung-Hoon Ahn[1]

Received: 6 March 2019 / Revised: 16 August 2019 / Accepted: 8 September 2019 / Published online: 29 October 2019

Abstract

Artificial muscle is one of the more prominent topics in modern robotics as it can be applied to robotic arms, electric vehicles and wearable robots (Shahinpoor et al. in Smart Mater Struct 7:15–30, 1998; Jani et al. in Mater Des 56:1078–1113, 2014). The advantages of Shape Memory Alloy (SMA) artificial muscle are lightness and high energy density. The high energy density allows the actuator to make powerful motions. Meanwhile, SMA wire contracts 6% of its length, which means that the required displacement cannot be achieved by a simple connection. To resolve these disadvantages, the SMA wires are coiled in a diamond-shaped structure. If the electric current is given by contracting wires in the longitudinal direction, the actuator can exert force and displacement in the diagonal direction. As the crossed tendon finds its minimal length when actuated, the rotation angle converges to 90°. Parameters related with the rotating motion were selected, such as SMA wires' diameter and length, distance between the crossed part and elbow part, size of the diamond-shaped structure, friction, etc. To determine the maximum force of the actuator, a graphical method was used, which is similar to the yield strength determination (0.2% offset). Because the robotic elbow joint is connected by the tendon, the connections between links are flexible, and without motor it does not generate any sound or noise during operation. The robotic elbow joint using the SMA actuator is designed and analyzed, which can rotate 86.7° and generates maximum 56.3 N force.

Keywords Shape memory alloy · Tendon-driven · Robotic elbow joint

✉ Sung-Hoon Ahn
ahnsh@snu.ac.kr

Hyung-Bin Park
hb1234.park@gmail.com

Dong-Ryul Kim
kryul@snu.ac.kr

Hyung-Jung Kim
hjkim81@snu.ac.kr

Wei Wang
davidwang@hanyang.ac.kr

Min-Woo Han
mwhan@dgu.edu

[1] Department of Mechanical and Aerospace Engineering, Seoul National University, 1, Gwanak-ro, Gwanak-gu, Seoul 08826, Republic of Korea

[2] Department of Mechanical and Aerospace Engineering, Dongguk University, 30, Pildong-ro 1-gil, Jung-gu, Seoul 04620, Republic of Korea

[3] Department of Mechanical Engineering, Hanyang University, 222, Wangsimni-ro, Seongdong-gu, Seoul 04763, Republic of Korea

1 Introduction

The human elbow joint rotation mechanism is actuated by four major parts: muscles, cartilage, ligaments, and tendons. When the muscle shrink in length by 20–40% of its original length, the tendon pulls up the lower bones. Then, the rotation occurs along the cartilage while the ligaments hold the upper bone and lower bone not to be detached when rotating. The contraction length of the muscles is important for the rotation of this entire mechanism. Fortunately, human muscles can shrink in length from 20 to 40%, so that arms can bend 90° (Fig. 1).

However, many researchers have studied artificial muscles using ionic polymer-metal composites (IPMCs), piezoelectric polymers (PZTs), and shape memory alloys (SMAs). IPMCs are active actuators that show large deformation when low voltage is applied and low impedance is exhibited [1–4]. They can be modeled as capacitive and resistive actuators that behave like biological muscles and are useful in actuation as artificial muscles for biomechanics and biomimetics applications [1, 3].

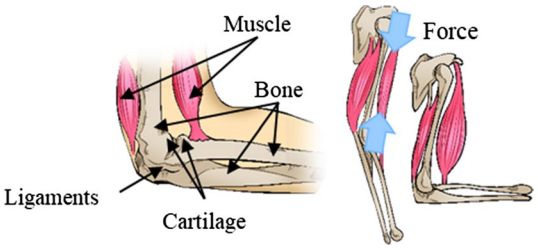

Fig. 1 Human elbow joint and lift-up motion

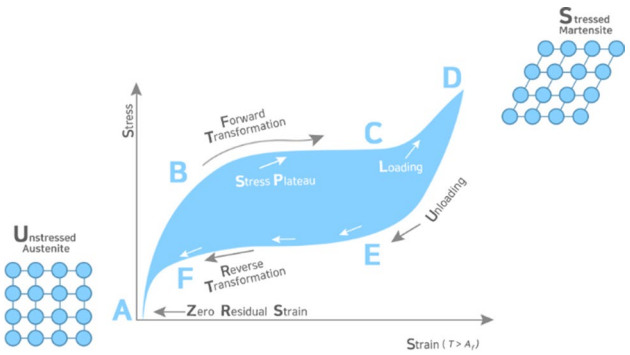

Fig. 2 Loop of superelasticity property of shape memory alloy

In this paper, the shape memory alloy wire was used for the actuating material and has the largest actuation stress in company with large strain among smart materials.

Shape memory alloys are a group of metal alloys that exhibit the characteristics of either large recoverable strains or large force due to temperature and/or load changes widely used in softrobotics for the continuous surface actuation [5–14]. In this research, the SMA wire is used for the longitudinal actuation.

The unique thermomechanical property of SMAs is due to the phase transformation from the austenite phase to martensite phase and vice versa. These transformations take place due to changes in the temperature, stress or a combination of both [15, 16].

When the SMA wire is heated beyond the activation temperature, it contracts due to the phase transformation from martensite to austenite as the temperature is raised using the resistive electrical (Joule) heating [17]. Thus, the shape memory effect, which is originated from the phase transformation, makes the actuation motion [15, 16].

When the SMA wire is in stress-induced martensite, high temperature and compete shape recovery transformations are observed on the material upon loading to austenite [15]. This property is called superelasticity and used to actuate the artificial muscle. Superelasticity, sometimes called pseudoelasticity, is an elastic (reversible) response to an applied stress caused by a phase transformation between the austenitic and martensitic phases of a crystal [15, 18]. As shown in Fig. 2, the graph

Table 1 Material properties of the shape memory alloy (SMA) [19]

Parameter	Description	Value
Young's modulus	Austenite (E_A)	75 GPa
	Martensite (E_M)	28 GPa
Phase transformation temperature	Austenite start (T_{As})	68 °C
	Austenite finish (T_{Af})	78 °C
	Martensite start (T_{Ms})	52 °C
	Martensite finish (T_{Mf})	42 °C
Specific heat capacity	C	0.322 J/g °C
Maximum deformation ratio	ε_{max}	8%

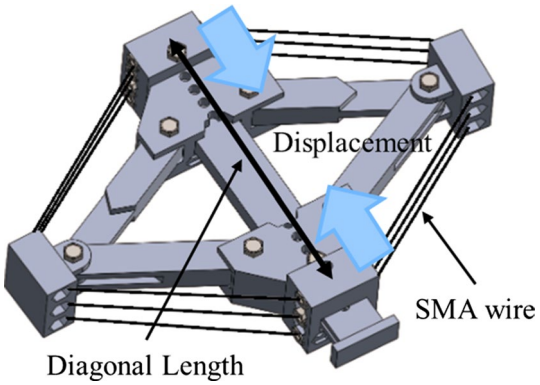

Fig. 3 Single diamond shaped actuator displacement

starts from Point A. When stress is induced to the SMA, it moves along from B to C and D. At Point D, with the loading, stressed martensite phase is dominant until it recovers to the original point through Points E and F.

The material properties of SMA wire is shown in Table 1, which is referenced from DYNALLOY, Inc and ref. 25 Table 1.

2 Design of Artificial Muscle Elbow Joint

2.1 Linear Actuator

An artificial muscle elbow joint design is proposed for precise actuation. The SMA wire is coiled up in a diamond shaped structure with 12 cm length sides that contract along the longitudinal direction when actuated. The actuator's links generate net force in the diagonal direction. Furthermore, slider lubricants are sprayed on the slider to make the motion smooth.

Unlike linear SMA wire arrangements, as shown in Fig. 3, the actuator can get the required displacement by the extra side length. Therefore, the actuator can get 2–3 times more linear displacement than linear longitudinal

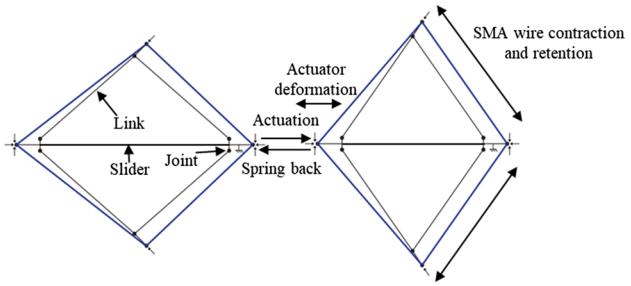

Fig. 4 Schematic diagram of the single diamond actuator's actuation deformation

connection in addition to easily stopping the actuator when the target displacement is achieved.

This structure facilitates actuators in multiplying the force by stacking up the coiled wire perpendicularly. In this design, the SMA wire is coiled up to 3 times for the larger force.

Deformation schematic diagram is shown in Fig. 4. As SMA wires contract and find their minimal length along the four sides, the actuator moves on the slider. As the actuator pulls the tendon attached to the end of the links, it moves along the longitudinal direction of the diamond shape.

2.2 Overall Design

The overall design is represented in Fig. 5. The lower arm consists of a single diamond shaped actuator for the higher force while the upper arm uses double diamonds for reducing the actuator width. The tendon wire connects the actuator with the elbow part located between two muscle actuators that fix the tendon from both sides.

When the actuator pulls the tendon, it finds its minimal length between the bolt and hole as in Fig. 5. These mechanisms generate the rotating motion.

However, the rotation angle can be adjusted by parameters like bolt and hole distance, distance between bolt and slider's neutral surface, and tendon wire stiffness. In this paper, the elbow joints are designed to achieve 45° angle each (Fig. 6).

2.3 Fabrication

All parts were fabricated with a 3D-printer. Stratasys F270 was used to prototype with ABS material.

While actuating, the SMA wire exerts up to 150 MPa and heat reaches 70 °C. The holes where the SMA wires pass through were reinforced by metallic materials to prevent heat fracture by the SMA wires.

The ball bearing was inserted for smooth movement in each joint.

3 Analysis of Elbow Joint

3.1 Actuation Force Measurement

Actuator force was measured by a 3-axis force sensor with a sensor accuracy of 1% (0.1 N) and maximum measuring force set at 250 N. The actuator's end is fixed on the surface

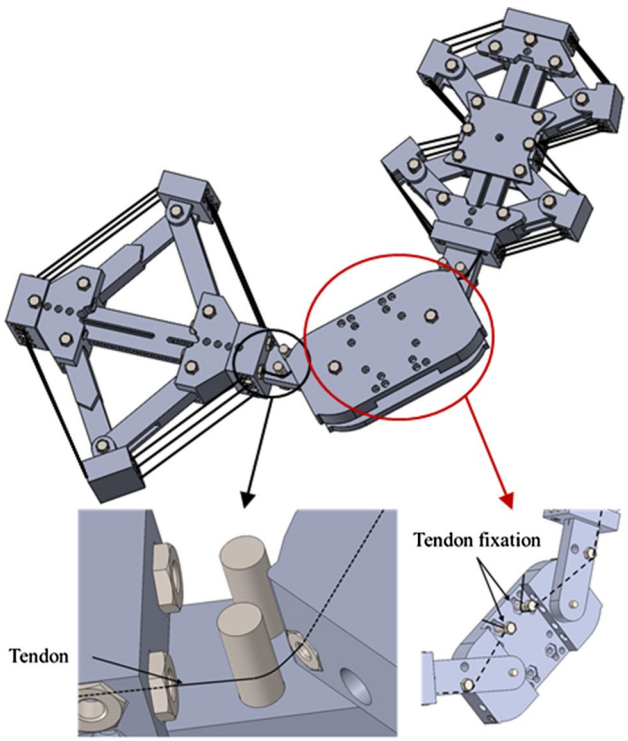

Fig. 5 Overall design and Tendon driven rotating motion

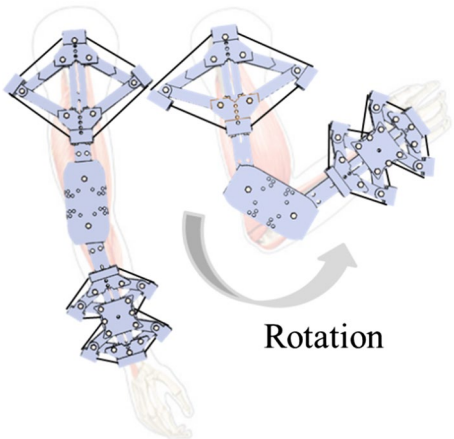

Fig. 6 Illustration of human elbow joint and robotic elbow joint

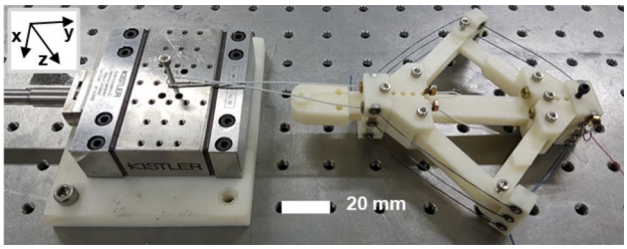

Fig. 7 Actuation force measurement by the 3-axis force sensor

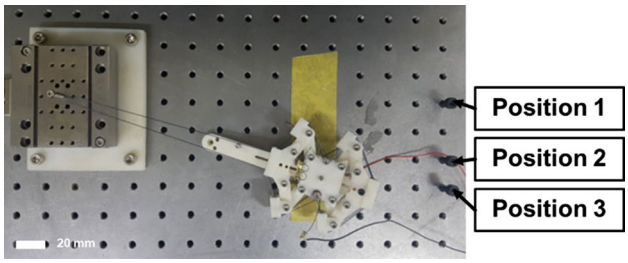

Fig. 8 Actuator configuration position

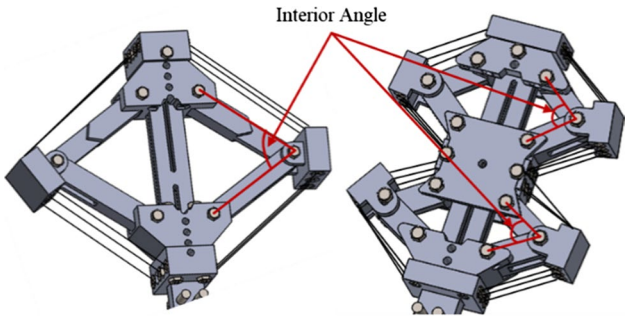

Fig. 9 Interior angle of the single diamond actuator and double diamond actuator

plate and the other side is fixed to pull the sensor. If the linear actuator pulls the tendon wire, the bolt fixed to the sensor head is followed by the wire (Fig. 7).

The actuator is fixed on the surface plate at three different positions, as shown in Fig. 8. With the positions, interior angles of the actuator are varied. This setting is intended for measuring the result pulling force with the interior angle of the actuator.

The pulling force is related to the actuator's interior angle, shape, given electric current, SMA wire length and diameter. In this paper, the pulling force is measured with the interior angle, shape and given electric current (Fig. 9).

3.2 Determination of Maximum Force

The maximum force value from the data is not obvious due to the sensor drift and the actuator's actuation characteristics.

The graphical method was used to solve this problem, which is similar to the yield strength determination (0.2% offset). The steepest gradient is calculated from the force data and used as a slope of the offset line, which starts at the offset time from the steepest gradient point of the force data. The actuation force data and offset line's intersection point is selected as the maximum force value.

$$Offset\ liney = a\left(x - x_1\right) + y_1$$

$$a = Steepest\ gradient\ from\ the\ force\ data;$$

$$x_1 = Origin\ x\ coordinate\ of the offset line;$$

$$y_1 = Origin\ y\ coordinate\ of\ the\ offset\ line$$

The x_1 and y_1 points are determined arbitrarily considering the total actuation time and the peak force. In determining the x_1 and y_1 points, the peak force of the actuator was considered due to the phase transformation time on high stress, which is related with the phase transformation propagation. If the peak force is high, the offset line moves to the $+$x direction. On the contrary, if the peak force is low, the offset line moves to the $-$x direction.

As shown in Figs. 10 and 11, the maximum force is determined by the intersection point from the force data and offset line.

The measured force data is summarized in Table 2 where the single strand of coiled actuator can exert a linear force with maximum 44.4 N when 2.0 A current is given. If the double strands of the SMA wire with the same diameter were used, the force would be measured as 56.3 N at maximum. However, the double diamond shape actuator can exert 50.0 N, although it is coiled up with a single strand of SMA wire since the double diamond actuator has more efficient SMA wire paths than a single diamond.

The SMA wire shows special properties when large stress is induced at the hinge joint, such as superelasticity and phase transformation propagation. In this regard, the double diamond actuator has a more efficient design than a single diamond actuator.

4 Test of Arm with Joint and Gripper

4.1 Experiment System

The experimental setup of the robotic elbow joint is represented in Fig. 12. The single diamond shaped actuator and double diamond shaped actuator were assembled for the

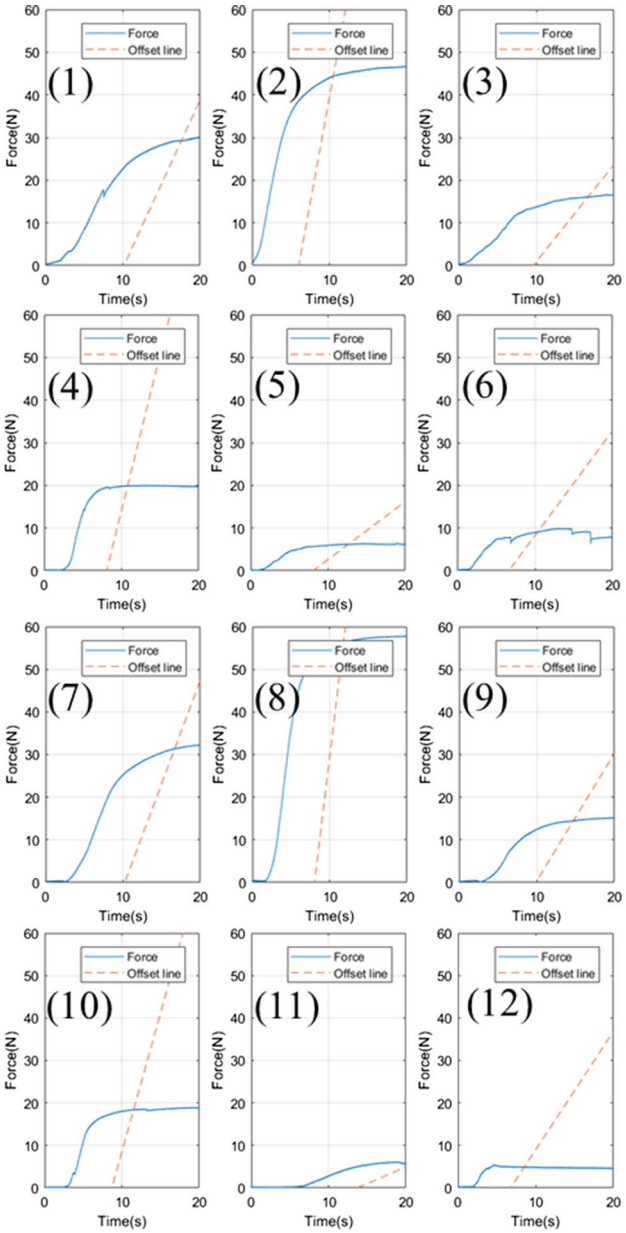

Fig. 10 Actuation force and offset line graph [from the left (1), (2), (3), (4), (5), (6), (7), (8), (9), (10), (11), (12)]

pulling actuation of the tendons in each direction. When the actuators pull the tendon, the elbow part makes the rotate motion according to the design parameters. And the DC motor was installed for the yaw rotation.

4.2 Experiment Process

The experiment process consists of four parts, as shown in Fig. 13.

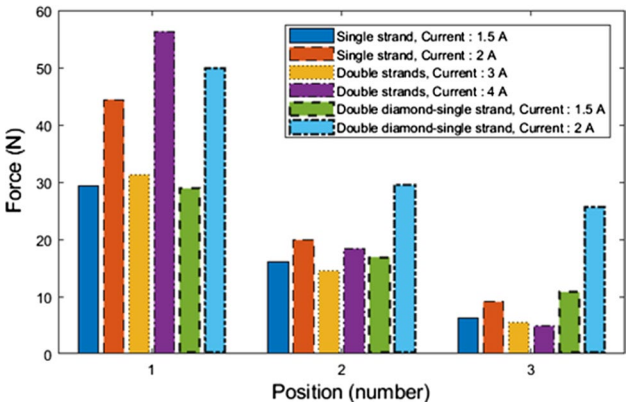

Fig. 11 Actuation force with the position and current

At the initial configuration in (a), each of the parts is arranged in horizontal direction. In (b), gripping the 200 g ball, the Smart Soft Composite (SSC) gripper forms a continuous curvature surface. In (c) the single diamond and double diamond actuators pull the tendon in each direction and the elbow part makes the rotating motion by the tendon driven mechanism. In (d) the DC motor attached to the surface plate rotates the robotic elbow joint to the opposite side.

5 Conclusions

The main purpose of this paper is to design and analyze the robotic elbow joint actuator.

- Design was focused on efficiency and precision.
- Analysis was focused on the actuation force.

The robotic elbow joint actuator design was newly introduced in this paper. The design aims to rotate 90°. Furthermore, the rotation angle can be modified by the design parameters.

The actuation forces were measured through the 3-axis force sensor. Although maximum force was not clear on the experiment, a graphical method for determining the maximum force of the actuator is suggested.

This actuator has many advantages compared to other actuators.

1. Light and simple:
   - 199 g, with no electric motor.
2. Large force:
   - The actuator can exert 56.3 N with a single diamond double strands of SMA wire.
3. Flexible and silent:
   - As the actuators connected by tendon, connections between elbow joint links are flexible and silent.

Table 2 Actuation force measurements of the linear actuator

SMA connection (diameter, length)	Configuration	Ampere (A)	Volt (V)	Watt (W)	Force (N)	Interior angle (°)	Graph number (#)
Single diamond Single strand (500 μm, 1065 mm)	Position 1	1.5	8.6	12.9	29.3	61.7	(1)
		2.0	11.2	22.4	44.4	59.4	(2)
	Position 2	1.5	8.4	12.6	16.1	48.7	(3)
		2.0	11.0	22.0	19.9	46.9	(4)
	Position 3	1.5	8.1	12.15	6.2	42.2	(5)
		2.0	10.7	21.4	9.1	42.0	(6)
Single diamond Double strands (500 μm, 2130 mm)	Position 1	3.0	9.0	27.0	31.3	74.7	(7)
		4.0	11.9	47.6	56.3	72.9	(8)
	Position 2	3.0	8.8	26.4	14.5	68.2	(9)
		4.0	11.7	46.8	18.4	66.1	(10)
	Position 3	3.0	8.5	25.5	5.5	66.7	(11)
		4.0	11.5	46.0	4.9	65.5	(12)
Double diamond Single strand (500 μm, 1155 mm)	Position 1	1.5	8.8	13.2	28.9	78.1 57.3	–
		2.0	11.4	22.8	50.0	83.6 40.3	–
	Position 2	1.5	8.8	13.2	16.9	55.8 40.1	–
		2.0	11.4	22.8	29.5	42.4 40.1	–
	Position 3	1.5	8.8	13.2	10.8	40.1 42.3	–
		2.0	11.4	22.8	25.6	52.0 37.1	–

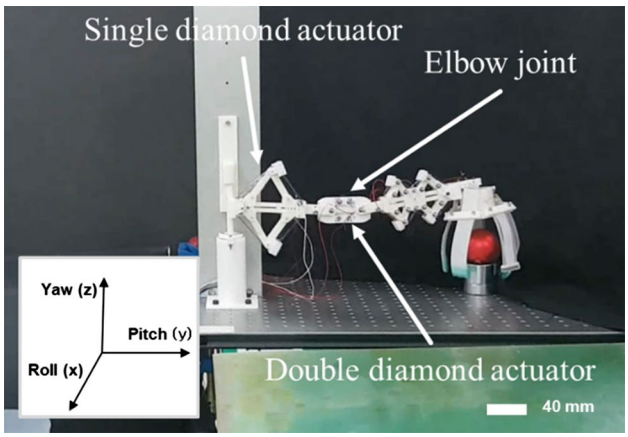

Fig. 12 Experimental setup of the robotic elbow joint

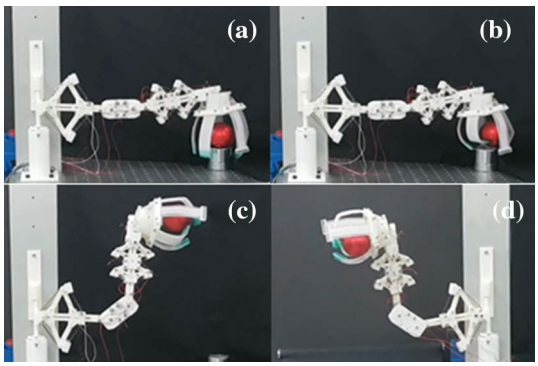

Fig. 13 200 g ball moving by the robotic elbow joint **a** initial configuration, **b** gripping the ball, **c** lifting up the ball, **d** moving the ball to the opposite side

From the experiment results, this actuator can exert 56.3 N whose magnitude of the force is greater comparing to other smart actuators. And compared to electric motors, this actuator has better properties, such as actuation force, weight and energy consumption. But actuation speed remains a problem to be solved. It takes 3–5 s to lift up and 8–12 s to lay down. To achieve faster lift up and lay down motion, it is needed to boost cooling SMA wire.

A robotic elbow joint using the SMA actuator is designed and analyzed in this research. Because the

connections between links are flexible and silent while actuating, the environment will be more comfortable. In addition, the robotic elbow joint can be applied to robotic arms, electric vehicles and wearable robots.

Acknowledgements This research was supported by a grant to Bio-Mimetic Robot Research Center Funded by Defense Acquisition Program Administration, and by Agency for Defense Development (UD190018ID), the National Research Foundation of Korea (NRF) funded by the MSIT (NRF-2018R1A2A1A13078704), the Basic Research Lab Program through the National Research Foundation of Korea (NRF) funded by the MSIT (2018R1A4A1059976), and Institute of Engineering Research, Seoul National University.

References

1. Shahinpoor, M., Bar-Cohen, Y., Simpson, J. O., & Smith, J. (1998). Ionic polymer-metal composites (IPMCs) as biomimetic sensors, actuators and artificial muscles: a review. *Smart Materials and Structures, 7,* 15–30.
2. Hunter, I. W., & Lafontaine, S. (1992). A comparison of muscle with artificial actuators. In: *IEEE, solid-state sensor and actuator workshop 5th technical digest*.
3. Chu, W. S., et al. (2012). Review of biomimetic underwater robots using smart actuators. *International Journal of Precision Engineering and Manufacturing, 13,* 1281–1292.
4. Binayak Bhandari, Gil-Yong Lee, Sung-Hoon Ahn, (2012) A review on IPMC material as actuators and sensors: Fabrications, characteristics and applications. International Journal of Precision Engineering and Manufacturing 13(1):141–163
5. Brinson, L. C., & Huang, M. S. (1996). Simplification and comparisons of shape memory alloy constitutive models. *Journal of Intelligent Material Systems and Structures, 7,* 108–114.
6. Elahinia, M. H., & Ahmadian, M. (2005). An enhanced SMA phenomenological model: The shortcomings of the existing models. *Smart Materials and Structures, 14,* 1297–1308.
7. Elahinia, M. H., & Ahmadian, M. (2005). An enhanced SMA phenomenological model: The experimental study. *Smart Materials and Structures, 14,* 1309–1319.
8. Brinson, L. C. (1993). One-dimensional constitutive behavior of shape memory alloys: Thermomechanical derivation with non-constant material functions and redefined martensite internal variable. *Journal of Intelligent Material Systems and Structures, 4,* 229–242.
9. Lagoudas, L., Hartl, D., Chemisky, Y., Machado, L., & Popov, P. (2012). Constitutive model for the numerical analysis of phase transformation in polycrstalline shape memory alloys. *International Journal of Plasticity, 32–33,* 155–183.
10. Rodrigue, H., et al. (2014). Cross-shaped twisting structure using SMA-based smart soft composite. *International Journal of Precision Engineering and Manufacturing-Green Technology, 1,* 153–156.
11. Kim, H. I., Han, M. W., Song, S. H., & Ahn, S. H. (2016). Soft morphing hand driven by SMA tendon wire. *Composites Part B Engineering, 105,* 138–148.
12. Rodrigue, H., Wang, W., Bhandari, B., Han, M. W., & Ahn, S. H. (2015). SMA-based smart soft composite structure capable of multiple modes of actuation. *Composites Part B Engineering, 82,* 152–158.
13. Wang, W., Rodrigue, H., et al. (2016). Soft composite hinge actuator and application to compliant robot gripper. *Composites Part B Engineering, 98,* 397–405.
14. Song, S. H., Lee, H., Lee, J. G., Lee, J. Y., Cho, M., & Ahn, S. H. (2016). Design and analysis of a smart soft composite structure for various modes of actuation. *Composites Part B Engineering, 95,* 155–165.
15. Tanaka, K., Kobayashi, S., & Sato, Y. (1986). Thermomechanics of transformation pseudoelasticity and shape memory effect in alloys. *International Journal of Plasticity, 2,* 59–72.
16. Porter, D. A., & Easterling, K. E. (1992). *Phase transformations in metals and alloys*, 2 edn, pp. 1–57.
17. Mincheol Kim, Yong-Jun Shin, Jang-Yeob Lee, Won-Shik Chu, Sung-Hoon Ahn, (2017) Pulse width modulation as energy-saving strategy of shape memory alloy based smart soft composite actuator. International Journal of Precision Engineering and Manufacturing 18(6):895–901
18. Kamita, T., & Matsuzaki, Y. (1998). One-dimensional pseudoelastic theory of shape memory alloys. *Smart Materials and Structures, 7,* 489–495.
19. DYNALLOY. Inc. (2018). *Flexinol actuator wire technical and design data*. Technical Info.

Hyung-Bin Park received his M.S. degree in 2018 from Seoul National University. His main research interests are Smart Materials, 3D-modeling and Computer Aided Design.

Dong-Ryul Kim is a Ph.D. candidate in the Department of Mechanical and Aerospace Engineering, Seoul National University. His main research interests include hybrid manufacturing process, soft robotics, and computer aided design.

Hyungjung Kim received his B.S.E. in automotive engineering from Kookmin University, Seoul, Korea, in 2004 and Ph.D. in mechanical engineering from Seoul National University (SNU), Seoul, Korea, in 2011. He is currently working as a senior engineer at Doosan Robotics. Before joining Doosan Robotics in 2019, he had worked as a senior research engineer at Doosan Infracore, Doosan Corp. and a postdoctoral researcher at SNU. His research interests include appropriate smart manufacturing, soft robotics, collaborative robots, machine tools, 3D printer, and machine learning.

Wei Wang is an Assistant professor at Hanyang University in Republic of Korea in the Department of Mechanical Engineering. He received his B.Eng. and M.S. degrees in 2008 and 2011 from Harbin Institute of Technology, respectively, and his Ph.D. from Seoul National University in 2016. His research interests include smart materials, bioinspired robotics, and soft robotics.

Min-Woo Han is an Assistant professor in the Department of Mechanical, Robotics and Energy Engineering, Dongguk University. He received his B.S.E. degree from the Dongguk University (2010), M.S. (2013) and Ph.D. degrees from Seoul National University (2017). His main research interests are soft robotics, smart materials, and innovate design.

Sung-Hoon Ahn is a Professor in the Department of Mechanical and Aerospace Engineering at Seoul National University (SNU). He received his B.S.E. degree from the University of Michigan (1992), M.S. (1994) and Ph.D. degrees from Stanford University (1997). His research topics include smart factory, 3D printing, nano fabrication, soft robotics, and appropriate technology.